

Supporting Information

Intrinsic Superoxide Dismutase Activity of MnO Nanoparticles Enhances Magnetic Resonance Imaging Contrast

Ruben Ragg,^a Anna M. Schilmann,^a Karsten Korschelt,^a Christian Wieseotte,^b Martin Klueker,^a Melanie Viel,^a Lara Völker,^a Sebastian Preiß,^a Jana Herzberger,^{c,d} Holger Frey,^c Katja Heinze,^a Peter Blümler,^e Muhammad N. Tahir,^a Filipe Natalio,^f and Wolfgang Tremel^{a*}

^a Institute of Inorganic and Analytical Chemistry, Johannes Gutenberg University Mainz, Duesbergweg 10–14, 55128 Mainz, Germany. * email: tremel@uni-mainz.de

^c Section of Medical Physics, University Medical Center, Johannes Gutenberg University Mainz, Langenbeckstr. 1, 55131 Mainz, Germany.

^c Institute of Organic Chemistry, Johannes Gutenberg University Mainz, Duesbergweg 10–14, 55128 Mainz, Germany.

^d Graduate School Materials Science in Mainz, Staudinger Weg 9, 55128 Mainz, Germany.

^e Institute of Physics, Johannes Gutenberg University Mainz, Staudingerweg 7, 55128 Mainz, Germany.

^f Institute of Chemistry - Inorganic Chemistry, Kurt Mothes-Str. 2, Martin-Luther-Universität Halle-Wittenberg, 06120 Halle, Germany.

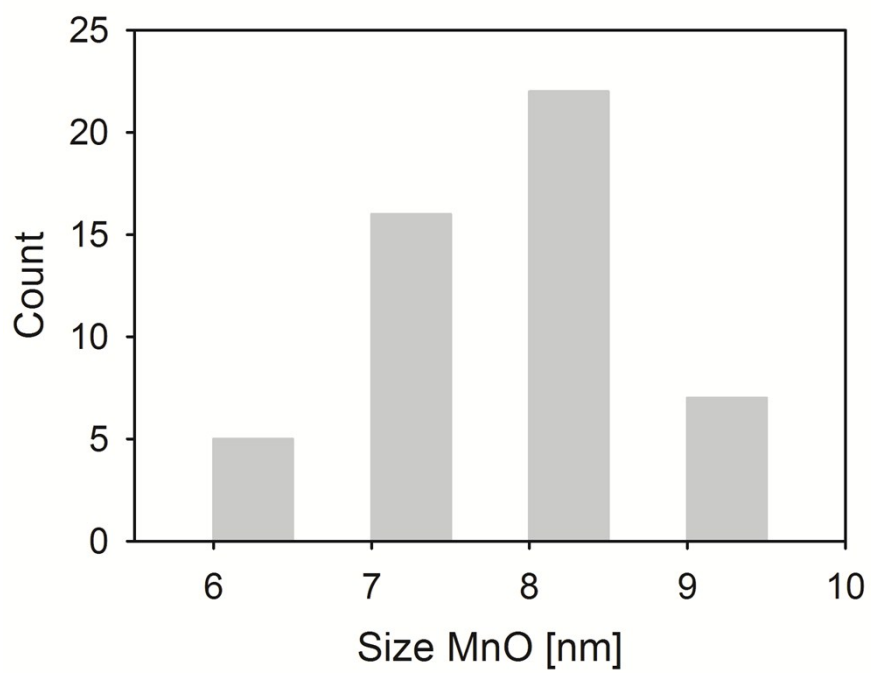


Fig. S1. Size distribution for MnO NPs determined by TEM (size of 50 individual NPs), revealing an average diameter of 7.6 ± 0.7 nm.

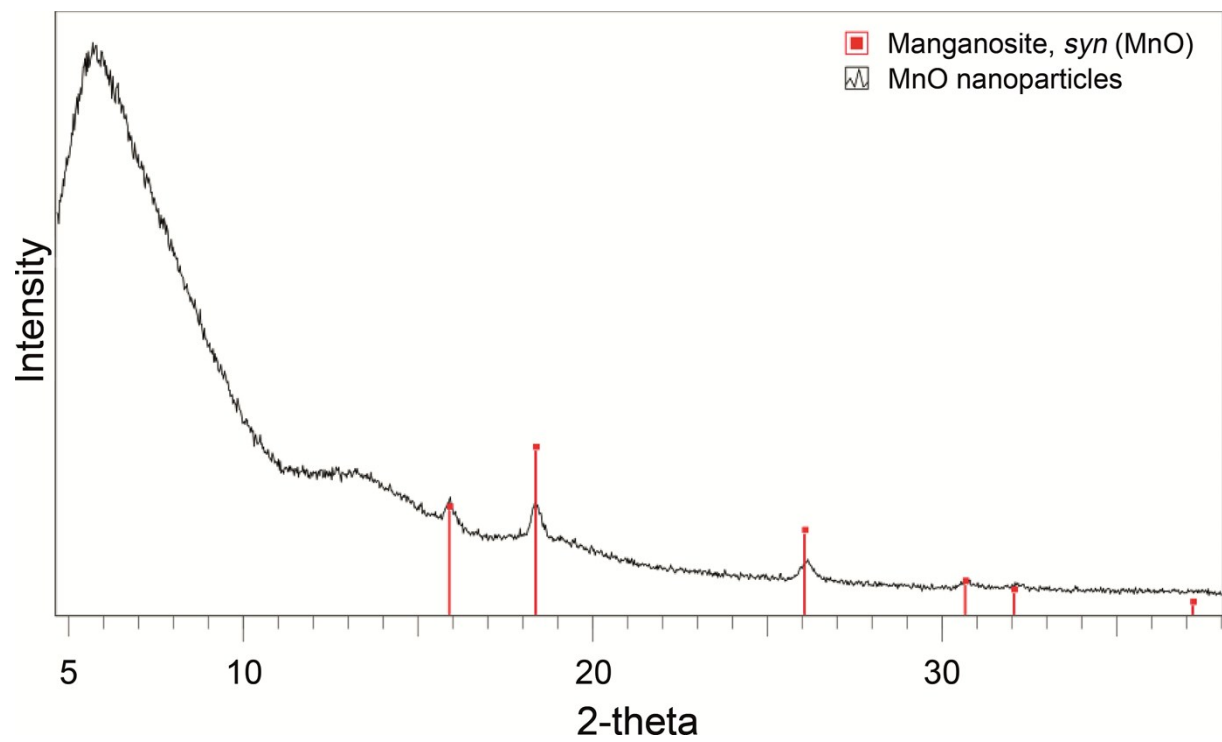


Fig. S2. P-XRD of MnO NPs (black) showing the formation of phase-pure face-centered cubic manganosite, *syn*-MnO (red).

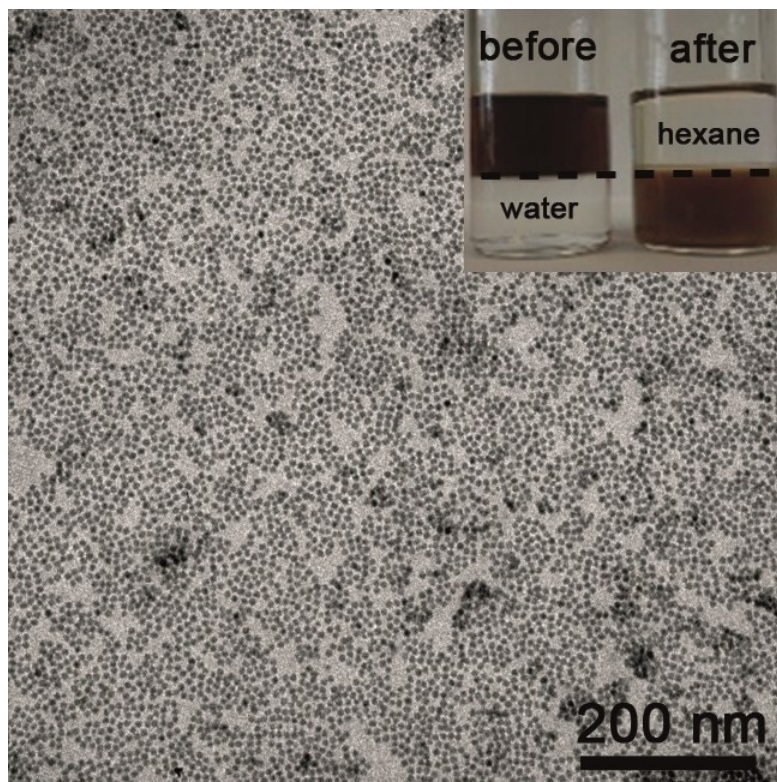


Fig. S3. Water soluble surface functionalized 8 nm MnO NPs with C-PEG. NPs retain size and shape during the functionalization process. Scale bar: 200 nm. Inset: Phase transfer of the MnO NPs in hexane/water before (left) and after (right) the functionalization with C-PEG.

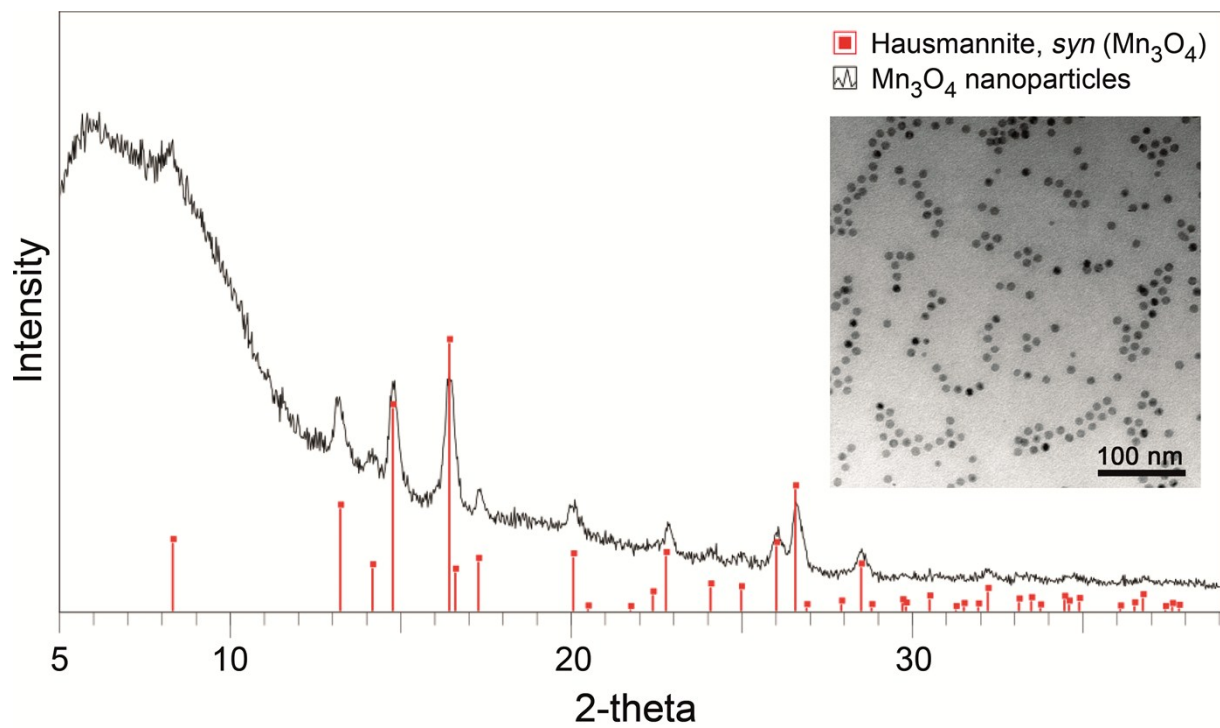


Fig. S4. Synthesis of Mn₃O₄ NPs. P-XRD of Mn₃O₄ NPs (black) showing the formation of phase-pure body-centered tetragonal hausmannite, *syn*-Mn₃O₄ (red). Inset: TEM Image of monodisperse 8 nm Mn₃O₄ NPs. Scale bar: 100 nm.

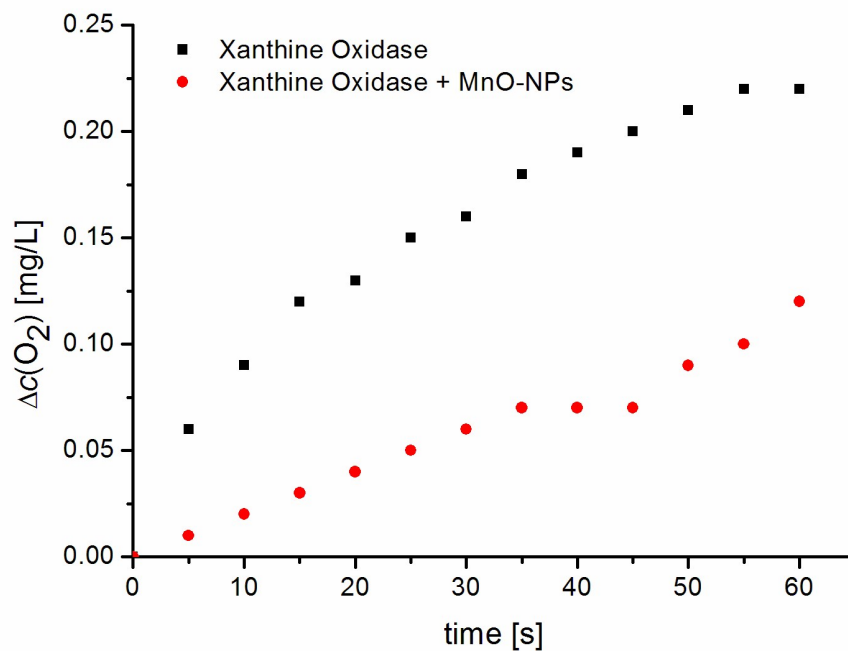


Fig. S5. Oxygen evolution of MnO NPs when exposed to superoxide radicals generated by xanthine/xanthine oxidase (XO) without addition of cytochrome c (pH 7.4). Molecular oxygen (O_2) is depleted by enzymatic activity of XO (black) forming superoxide radicals. In general superoxide dismutation by SOD-active materials leads to the formation of hydrogen peroxide and oxygen (50% each). MnO NPs reduce the oxygen depletion to approx. 50% (red), which is equivalent to the formation of an equivalent amount of O_2 .

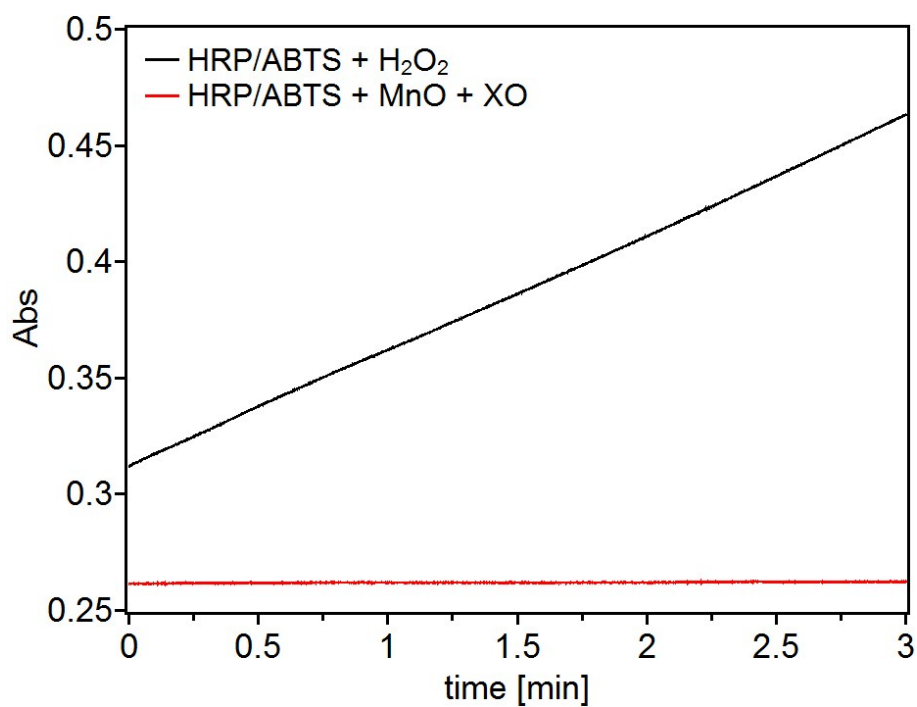


Fig. S6. Formation of H₂O₂ during the SOD-reaction of MnO NPs (red) cannot be demonstrated using the classical HRP/ABTS assay due to the intrinsic catalase-like activity of MnO NPs. As a positive control H₂O₂ has been added to the reaction mixture without addition of MnO (black).

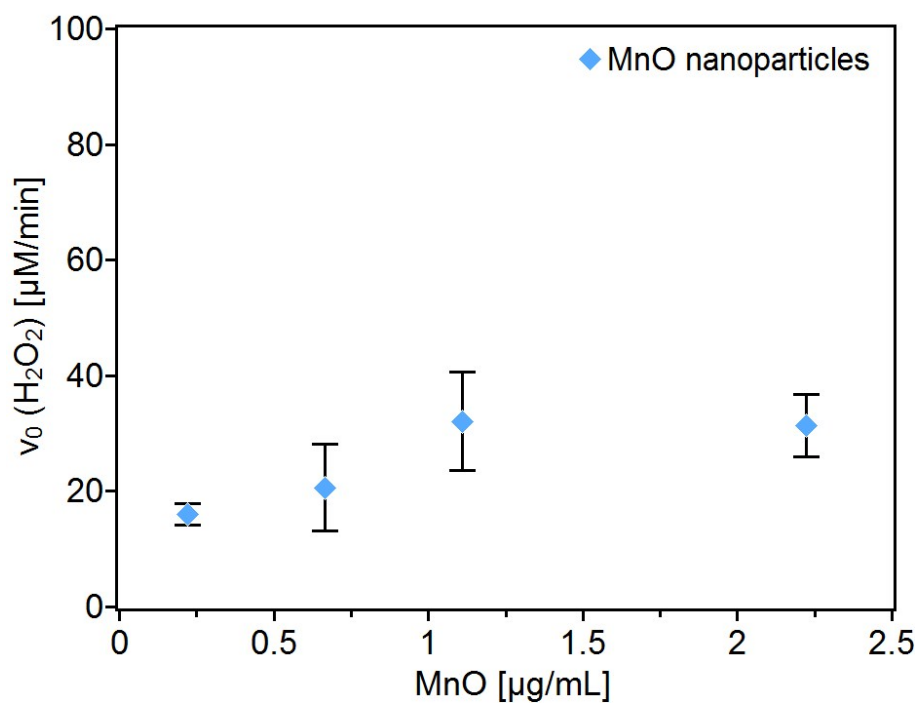


Fig. S7. Catalase-like reaction of MnO NPs monitored by disappearance of peroxide at 240 nm for 3 min at RT. Concentrations of 10mM H₂O₂ and 50 mM PBS pH 7.4 were used, while varying amounts of MnO nanoparticles (0.2, 0.7, 1.1, 2.2 µg/mL).

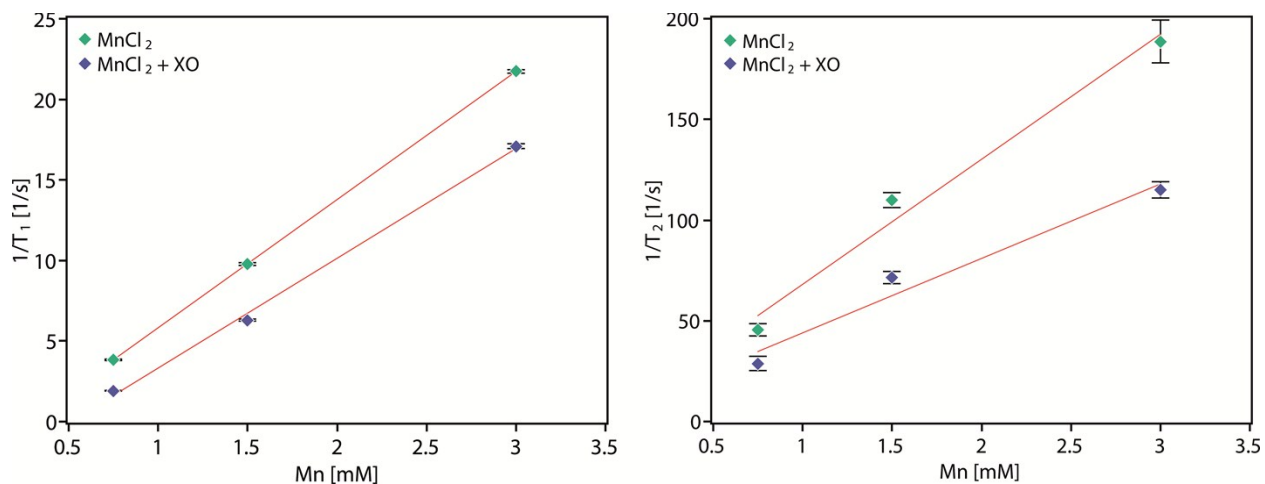


Fig. S8. Specific relaxivities r_1 and r_2 of Mn^{2+} ion a without and b with addition of superoxide generated by xanthine/xanthine oxidase (XO). Relaxivities were determined by linear regression and show values for **a** $r_1 = 7.95 \pm 0.01 \text{ mM}^{-1}\text{s}^{-1}$ and $r_2 = 62.07 \pm 8.26 \text{ mM}^{-1}\text{s}^{-1}$, **b** $r_1 = 6.81 \pm 0.34 \text{ mM}^{-1}\text{s}^{-1}$ and $r_2 = 36.95 \pm 6.88 \text{ mM}^{-1}\text{s}^{-1}$, respectively.

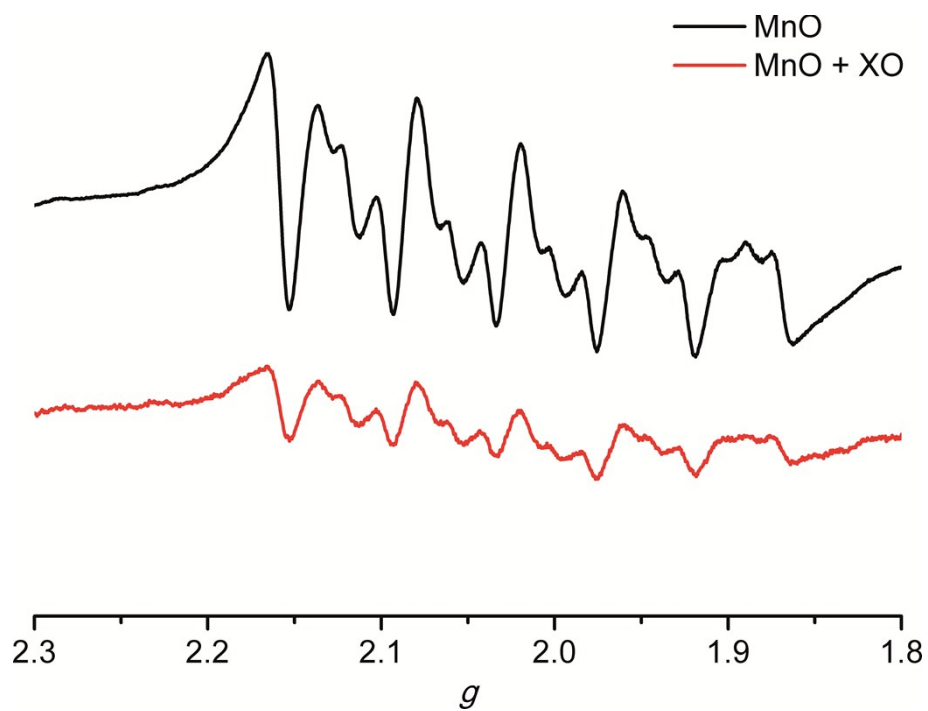


Fig. S9. X-band EPR spectra of MnO NPs in a frozen 50/50 mixture water/glycerol (77 K, 9.4 GHz) without (black) and with addition of superoxide generated by xanthine/xanthine oxidase (XO, red) after 30 min. Both spectra show the characteristic anisotropic six line pattern of Mn²⁺ (⁵⁵Mn; $I = 5/2$; 100%) with a reduction in signal intensity due to the superoxide treatment (red).